Please cite this article in press as: Hippenmeyer et al., Mosaic Analysis with Double Markers Reveals Cell-Type-Specific Paternal Growth Dominance, Cell Reports (2013), http://dx.doi.org/10.1016/j.celrep.2013.02.002

Cell Reports
Resource

Mosaic Analysis with Double Markers Reveals Cell-Type-Specific Paternal Growth Dominance

Simon Hippenmeyer,[1,2,*] Randy L. Johnson,[3] and Liqun Luo[1,*]
[1]Howard Hughes Medical Institute and Department of Biology, Stanford University, Stanford, CA 94305, USA
[2]IST Austria (Institute of Science and Technology Austria), 3400 Klosterneuburg, Austria
[3]Department of Biochemistry and Molecular Biology, University of Texas, MD Anderson Cancer Center, Houston, TX 77030, USA
*Correspondence: simon.hippenmeyer@ist.ac.at (S.H.), lluo@stanford.edu (L.L.)
http://dx.doi.org/10.1016/j.celrep.2013.02.002

SUMMARY

Genomic imprinting leads to preferred expression of either the maternal or paternal alleles of a subset of genes. Imprinting is essential for mammalian development, and its deregulation causes many diseases. However, the functional relevance of imprinting at the cellular level is poorly understood for most imprinted genes. We used mosaic analysis with double markers (MADM) in mice to create uniparental disomies (UPDs) and to visualize imprinting effects with single-cell resolution. Although chromosome 12 UPD did not produce detectable phenotypes, chromosome 7 UPD caused highly significant paternal growth dominance in the liver and lung, but not in the brain or heart. A single gene on chromosome 7, encoding the secreted insulin-like growth factor 2 (IGF2), accounts for most of the paternal dominance effect. Mosaic analyses implied additional imprinted loci on chromosome 7 acting cell autonomously to transmit the IGF2 signal. Our study reveals chromosome- and cell-type specificity of genomic imprinting effects.

INTRODUCTION

In diploid organisms, most genes are expressed from both parental chromosomes. However, a subset of genes in mammals and plants is subject to a unique mode of regulation called genomic imprinting (Barlow, 2011; Bartolomei and Ferguson-Smith, 2011), whereby either the maternal or paternal allele is preferentially silenced. Genomic imprinting is essential for embryonic development in mammals (Barton et al., 1984; McGrath and Solter, 1984; Surani et al., 1984). Deregulation of imprinting has been implicated in many diseases, including cancer and brain disorders such as Angelman and Prader-Willi syndromes (Feinberg, 2007; Mabb et al., 2011; Nicholls and Knepper, 2001). Despite the importance of imprinting in controlling prenatal growth, behavior, and metabolism of the whole organism (Ferguson-Smith, 2011; Wilkinson et al., 2007), the functional relevance of imprinting at the cellular level is poorly understood for most genes.

The analysis of mice carrying uniparental disomy (UPD) of whole chromosomes (somatic cells with two copies of either the maternal or paternal chromosome), as well as duplication and deficiency of defined chromosomal regions, has been fundamental for the identification and mapping of imprinted chromosomal regions and loci in the mouse genome (Cattanach and Kirk, 1985; Williamson et al., 2013). However, phenotypic analysis of mice with UPD, deletions, and duplications is limited due to the lack of assays with cellular resolution. Only very recently, the analysis of paternally or maternally inherited mutations with concurrent cell marker labeling has begun to reveal tissue-specific physiological functions for certain imprinted genes (Ferrón et al., 2011; Garfield et al., 2011). Here, we use the mosaic analysis with double markers (MADM) system (Zong et al., 2005) to probe the effects of genomic imprinting at the whole-chromosome level and with single-cell resolution across many tissues and cell types in the mouse.

RESULTS AND DISCUSSION

MADM Can Assess Genomic Imprinting Phenotypes with Single-Cell Resolution

MADM can generate Cre/LoxP-dependent mitotic recombination between homologous chromosomes and at the same time label genetically defined progeny with distinct fluorescent markers. Specifically, mitotic recombination at G2 phase followed by X segregation of recombined chromosomes can produce fluorescently labeled progeny with chromosomal compositions distinct from parental cells (Zong et al., 2005). Even for chromosomes that do not harbor any mutations, G2-X events produce near-complete UPD for a particular chromosome carrying the MADM cassettes (Figures 1A and S1A). Consequently, imprinted genes located on such a chromosome will be homozygosed and either overexpressed by a factor of two or not expressed depending on their imprinting status. Furthermore, cells with unipaternal disomy are fluorescently labeled with GFP and sister cells with unimaternal disomy with tandem dimer Tomato (tdTomato), or vice versa (Figures 1A and S1A). Thus, MADM provides in principle a unique experimental platform to systematically assay the consequences of genomic imprinting at the whole-chromosome level by visualizing the single-cell phenotypes of defined UPDs in genetic mosaic animals.

Chromosome 7, but Not Chromosome 12, UPD Leads to Drastic Paternal Growth Dominance in the Liver

To test the potential effect of imprinted genes on specific chromosomes, we produced MADM cassettes for mouse chromosome 7

Please cite this article in press as: Hippenmeyer et al., Mosaic Analysis with Double Markers Reveals Cell-Type-Specific Paternal Growth Dominance, Cell Reports (2013), http://dx.doi.org/10.1016/j.celrep.2013.02.002

Cell PRESS
Open ACCESS

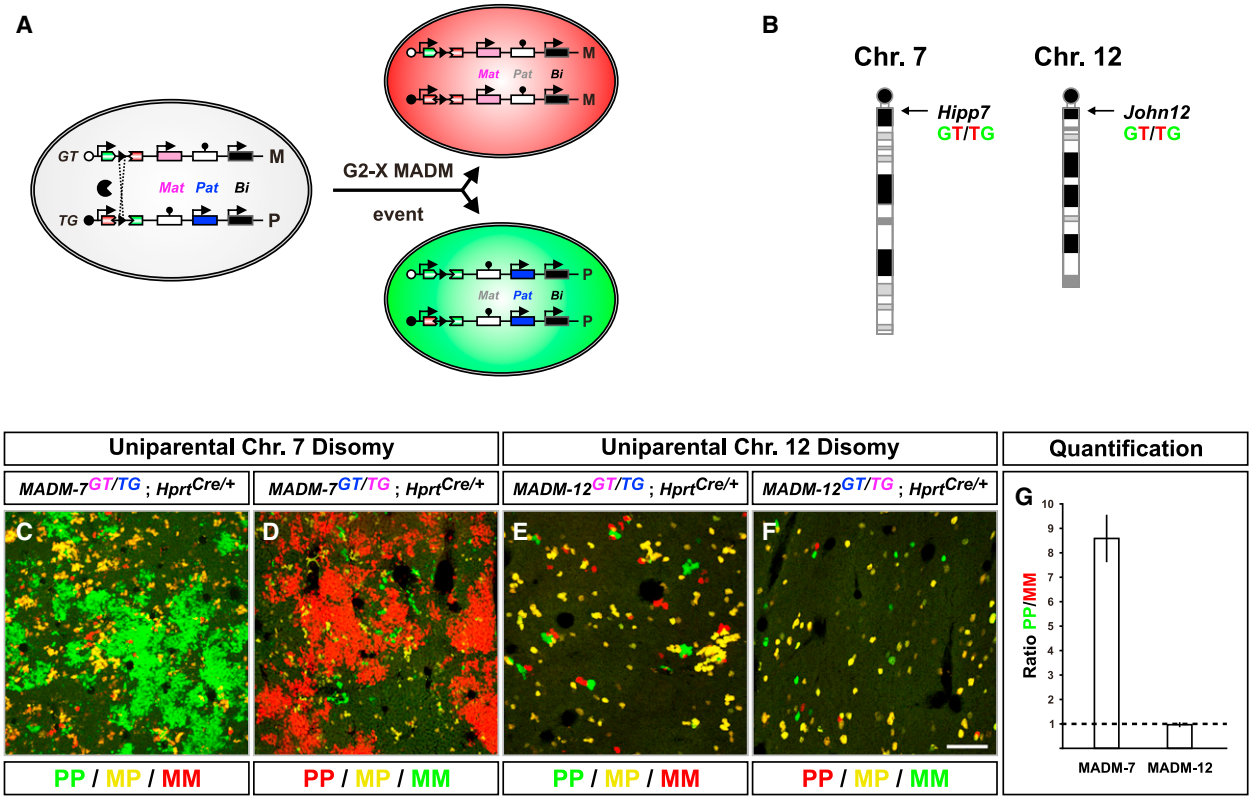

Figure 1. MADM Reveals a Chromosome-Specific Imprinting Phenotype with Single-Cell Resolution

(A) G2-X MADM events result in near-complete uniparental chromosomal disomy labeled in green (PP) and red (MM) fluorescent colors, respectively.

(B) Chromosomal location of *Hipp7* (chromosome 7) and *John12* (chromosome 12) genomic loci with inserted MADM cassettes.

(C and D) P21 livers from *MADM-7*$^{GT/TG}$;*Hprt-Cre*$^{+/-}$ mice with uniparental chromosome 7 disomy.

(E and F) P21 livers from *MADM-12*$^{GT/TG}$;*Hprt-Cre*$^{+/-}$ mice with uniparental chromosome 12 disomy.

(G) Quantification of the PP/MM ratios of liver UPD hepatocytes in cryosections in P21 *MADM-7*$^{GT/TG}$;*Hprt*$^{Cre/+}$ (MADM-7) and *MADM-12*$^{GT/TG}$;*Hprt*$^{Cre/+}$ (MADM-12; n = 16 from 3 individual male mice). Values represent mean ± SEM. For detailed methods of quantifying the PP/MM ratio in MADM-7 P21 liver, see also Figures 4 and S4.

Depending on whether the *GT* and *TG* alleles were introduced from the father (blue) or the mother (pink), unipaternal disomy cells are labeled in green (C and E) or in red (D and F) as indicated. Scale bar, 200 μm. See also Figure S1.

because mouse chromosome 7 is most enriched for imprinted genes and harbors several well-studied clusters of imprinted genes (Williamson et al., 2013). We inserted MADM cassettes near the centromere of chromosome 7 (Figures 1B and S1B; see Experimental Procedures for details) using a similar knockin strategy as previously described (Hippenmeyer et al., 2010). We then used a ubiquitous Cre driver (*Hprt-Cre*) to induce chromosome 7 UPD across the whole animal in a mosaic fashion. When using GFP to label unipaternal disomy cells (PP), we found a massive expansion of green hepatocytes in the liver (Figures 1C and 1G) when compared with unimaternal disomy cells (MM) labeled by tdTomato. In a separate experiment in which we switched colors of UPD cells (tdTomato for PP, and GFP for MM), we found that red hepatocytes expanded as a consequence of the chromosome 7 UPD (Figure 1D). Thus, unipaternal disomy of chromosome 7 leads to a massive expansion of hepatocytes when compared with unimaternal chromosome 7 disomy.

We also created MADM cassettes near the centromere of mouse chromosome 12 for mosaic analysis of candidate genes on that chromosome (Figures 1B and S1C). *Hprt-Cre* together with the MADM transgenes on chromosome 12 also produced chromosome 12 UPD cells in a mosaic fashion across the whole animal and including the liver. In contrast to chromosome 7 UPD, hepatocytes carrying either paternal or maternal chromosome 12 UPD appeared similar in number (Figures 1E–1G).

Imprinting Effects in Chromosome 7 UPD Display Cell-Type Specificity

We extended our analysis to additional tissues and cell types with mosaic chromosome 7 or chromosome 12 UPD. Qualitative (Figures 2A–2C and 2E–2G) and quantitative (Figure 2I) evaluation of hippocampal CA1 pyramidal neurons and cerebellar Purkinje cells in the brain, as well as cardiomyocytes in the heart, revealed no significant differences in cell number regardless of whether these cells carried unipaternal or unimaternal disomies for chromosome 7 or chromosome 12. By contrast, lung epithelia displayed a marked expansion of cells with unipaternal chromosome 7 but not chromosome 12 UPD (Figures 2D and 2H), similar

Cell PRESS
Open ACCESS

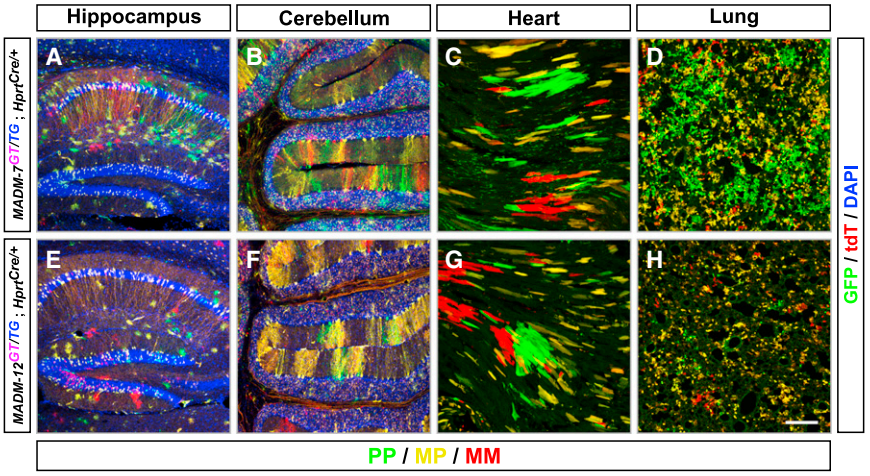

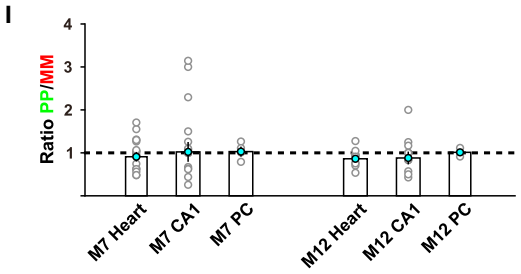

Figure 2. Cell-type-Specific Paternal Dominance of Chromosome 7 UPD

(A–H) MADM labeling of chromosome 7 (A–D) and chromosome 12 (E–H) in the hippocampus (A and E), cerebellum (B and F), heart (C and G), and lung (D and H) at P21. PP cells are green, and MM cells are red. DAPI stainings (blue) outline the general organization of the hippocampus (A and E) and cerebellum (B and F). Scale bar, 200 μm.

(I) Quantification of the ratios of green PP to red MM cells in cryosections: cardiomyocytes in the heart ([n = 16 for M7; n = 10 for M12] from male animals [n = 3 each]), CA1 pyramidal neurons in hippocampus ([n = 16 for M7; n = 11 for M12] from individual male animals [n = 3 each]), and Purkinje cells (PC) in cerebellum from entire male half-brains (n = 4 for M7 and n = 3 for M12). Individual data points as well as mean ± SEM are indicated. See also Figure S2.

to liver hepatocytes. We conclude that MADM-induced chromosome 7 but not chromosome 12 UPD results in cell-type-specific expansion with unipaternal disomy.

To exclude the possibility that the MADM markers on chromosome 7 themselves were selectively silenced due to imprinting, we generated mice containing constitutively expressed, reconstituted GFP (*Hipp7*$^{GG/+}$) and tdTomato (*Hipp7*$^{TT/+}$) markers, respectively, and intercrossed them to generate *Hipp7*$^{GG/TT}$ animals. All cells in every organ analyzed at postnatal day (P) 21 in *Hipp7*$^{GG/TT}$ expressed both markers uniformly (Figure S2). Therefore, the unequal ratio of hepatocytes and lung epithelia with unipaternal over unimaternal chromosome 7 UPD did not result from selective silencing of one marker in putative GFP$^+$/tdTomato$^+$ cells but reflects an imprinting phenotype whereby cells with unipaternal disomy have a growth advantage over unimaternal disomy.

Paternal Growth Advantage in Chromosome 7 UPD Commences during Embryogenesis

What is the developmental origin of cell number expansion in unipaternal chromosome 7 disomy? To address this question, we carried out a developmental time course analysis focusing on liver hepatocytes with MADM-induced chromosome 7 UPD. At embryonic day (E) 12, no expansion of the hepatocyte population with unipaternal disomy was apparent (Figure 3A). However, 4 days later at E16, unipaternal chromosome 7 disomy cells already outnumbered unimaternal chromosome 7 disomy cells (Figure 3B). We validated this result by clonal analysis using tamoxifen (TM)-induced CreER (Figures 3J and 3K). In liver clones induced at E12, the size of clone-harboring PP cells already exceeded that of MM by more than 2-fold by E16. These findings are consistent with previous reports showing that the embryonic liver has a remarkable capacity for growth (Stanger et al., 2007).

Expansion of the MADM-labeled domains with unipaternal chromosome 7 hepatocytes became more apparent at postnatal stages (Figures 3C–3F). Nevertheless, mosaic MADM-7 livers were neither larger than wild-type nor displayed any signs of tumors in mice of up to 6 months of age, suggesting that cell expansion due to unipaternal disomy still follows organ size control mechanism as in wild-type hepatocytes (Stanger, 2008). In contrast to hepatocytes with unipaternal chromosome 7 disomy, hepatocytes with either UPD for chromosome 12 displayed equal numbers postnatally up to 6 months (Figures 3G–3I).

Ablation of a Single Gene on Chromosome 7, *Igf2*, Largely Mitigates Paternal Growth Advantage of Chromosome 7 UPD

The paternal dominance of chromosome 7 disomy cells could, in principle, reflect the consequence of homozygosing many or just a few imprinted genes on chromosome 7. Because the "imprintome" of chromosome 7 in the liver is currently unknown, we pursued a candidate gene approach to identify the causal gene. Chromosome 7 harbors several clusters of imprinted genes that either promote or antagonize growth, including paternally expressed *Igf2* (*insulin-like growth factor 2*) (DeChiara et al., 1991), as well as maternally expressed *H19* (Bartolomei et al., 1991) and *Cdkn1c* (*cyclin-dependent kinase inhibitor 1C*, aka *p57*^{kip2}) (Hatada and Mukai, 1995; Matsuoka et al., 1995). The growth advantage of unipaternal disomy can be caused by overexpression of paternally expressed growth-promoting gene(s), absence of maternally expressed growth-antagonizing gene(s), or a combination of both. We began by assessing the involvement of *Igf2* and introduced a null allele from the father into our

Please cite this article in press as: Hippenmeyer et al., Mosaic Analysis with Double Markers Reveals Cell-Type-Specific Paternal Growth Dominance, Cell Reports (2013), http://dx.doi.org/10.1016/j.celrep.2013.02.002

Cell PRESS
Open ACCESS

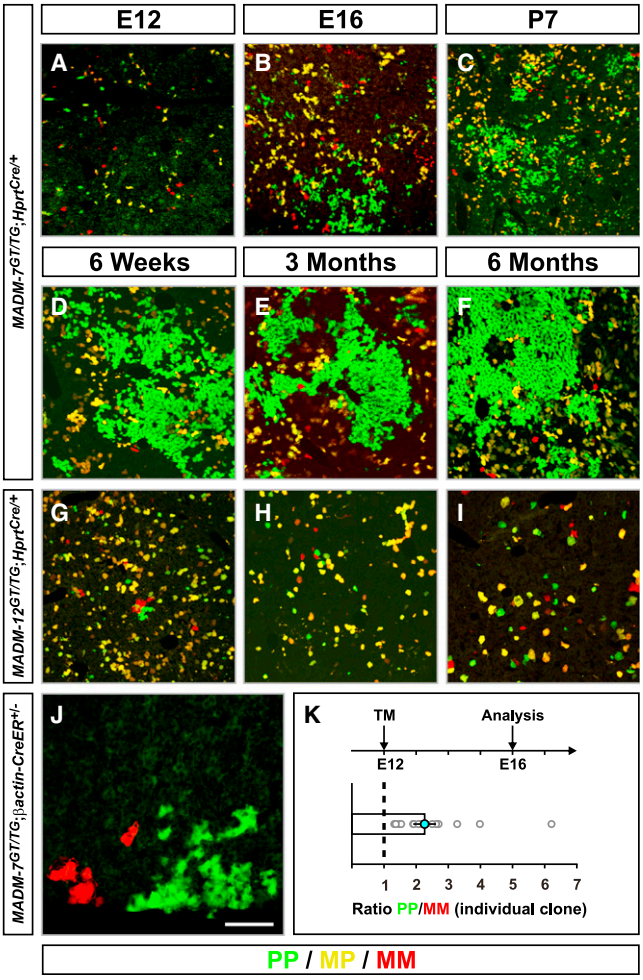

Figure 3. Paternal Dominance of Chromosome 7 UPD Initiates during Embryogenesis

(A–I) Time course analysis of liver at times indicated in *MADM-7*$^{GT/TG}$;*Hprt-Cre*$^{+/-}$ (A–F) and *MADM-12*$^{GT/TG}$;*Hprt-Cre*$^{+/-}$ (G–I).

(J and K) Clonal analysis in *MADM-7*$^{GT/TG}$;*βactin-CreER*$^{+/-}$ liver. (J) A representative image of a single G2-X MADM clone at E16 with TM injected at E12. Note the increased expansion of green PP when compared to red MM chromosome 7 cells. (K) Quantification of G2-X MADM clones. The mean ± SEM of the PP/MM ratio is 2.3 ± 0.3 (n = 15).

In all panels, PP cells are green, and MM cells are red. Scale bars, 180 μm (A), 200 μm (B), 250 μm (C), 300 μm (D–I), and 50 μm (J).

MADM analysis. Because *Igf2* is paternally expressed in most cells (DeChiara et al., 1991), *Igf2*$^{m/-}$ (*m* stands for the wild-type allele inherited from the mother) should in principle be equivalent to homozygous *Igf2*$^{-/-}$. Remarkably, we found a striking reduction of the large clusters of unipaternal chromosome 7 disomy cells at P21 in *Igf2*$^{m/-}$-MADM (Figures 4A and 4D compared with Figures 4B and 4E; Figures S3A and S3B).

To compare hepatocyte expansion with unipaternal chromosome 7 disomy produced by MADM in control mice and mice with paternal loss of *Igf2*, we quantified all green and red cells in entire liver sections to avoid selection bias and calculated their ratios (Figures 4G, S4A, and S4B). We found an 8.6- ± 0.9-fold paternal expansion in control-MADM. The PP/MM ratio was reduced to 2.2- ± 0.4-fold in animals with *Igf2*$^{m/-}$-MADM. To test whether the residual paternal dominance was due to IGF2 from a possible reactivation of the silenced maternal *Igf2* allele, or in serum from distinct sources not subjected to imprinting (DeChiara et al., 1991), we also examined the liver from homozygous *Igf2*$^{-/-}$ mutants with MADM labeling (Figures 4C and S3C). We found a reduction of the PP/MM ratio (Figure 4F) to the same level (2.1 ± 0.5) as when the *Igf2* mutation was introduced only from the father. By contrast, maternal transmission of the *Igf2* mutation had no effect on paternal dominance (Figures S3D, S4C, and S4D). Thus, the loss of the paternally inherited *Igf2* fully accounts for the imprinting effect.

To extend our findings to other tissues, we also examined the effect of IGF2 on the paternal growth dominance in the lung epithelia. We found that paternal transmission of the *Igf2* mutation also resulted in marked reduction of paternal growth dominance in the lung (Figures S4E–S4H), highlighting a general role of *Igf2* imprinting in distinct cell types. Taken together, these findings indicate that *Igf2* is a major factor driving unipaternal chromosome 7 growth dominance in the liver and lung.

Evidence that Additional Imprinted Factors on Chromosome 7 Act Cell Autonomously to Receive the IGF2 Signal

Although chromosome 7 harbors many imprinted genes controlling growth, we found that mutation of just one paternally expressed gene, *Igf2*, mitigates the majority of the paternal dominance effect. Our findings are in line with previous chimera studies implicating that duplication of distal chromosome 7 (where *Igf2* is located) and *Igf2* itself are responsible for causing overgrowth (Ferguson-Smith et al., 1991; McLaughlin et al., 1997). We further extended these studies with single-cell resolution by producing and visualizing UPD through rare mitotic recombination events enabled by MADM.

However, it is surprising that a secreted factor should be a major contributor in our experimental setting. Under the control-MADM-7 condition, all unipaternal disomy cells that overexpress *Igf2* originate from mitotic recombination events in a single cell and are surrounded by a vast majority of cells with regular paternal *Igf2* expression. Even with paternal growth dominance, unipaternal cells represent only a small fraction of the whole liver (see Figure S4A). We envision three possibilities to explain the paternal growth dominance that we observed in MADM-7 mice (Figure 4H). First, despite being a secreted factor, IGF2 acts predominantly cell autonomously. Furthermore, a 2-fold increase in IGF2 levels should greatly facilitate the growth of the unipaternal cells. We consider the first possibility unlikely because IGF2 is well known to bind IGF-binding proteins, enabling IGF2 distribution in the bloodstream and thus to signal growth of neighboring cells in paracrine and endocrine manners (Chao and D'Amore, 2008). Second, in addition to IGF2, another paternally expressed P factor acts cell autonomously to positively regulate IGF2 signal transmission. Again, this P factor should act in a dose-dependent fashion to account for the growth of unipaternal chromosome 7 disomy cells in a mostly wild-type background because it would also be present in 2-fold higher dosage levels, similar to IGF2. Third, a maternally

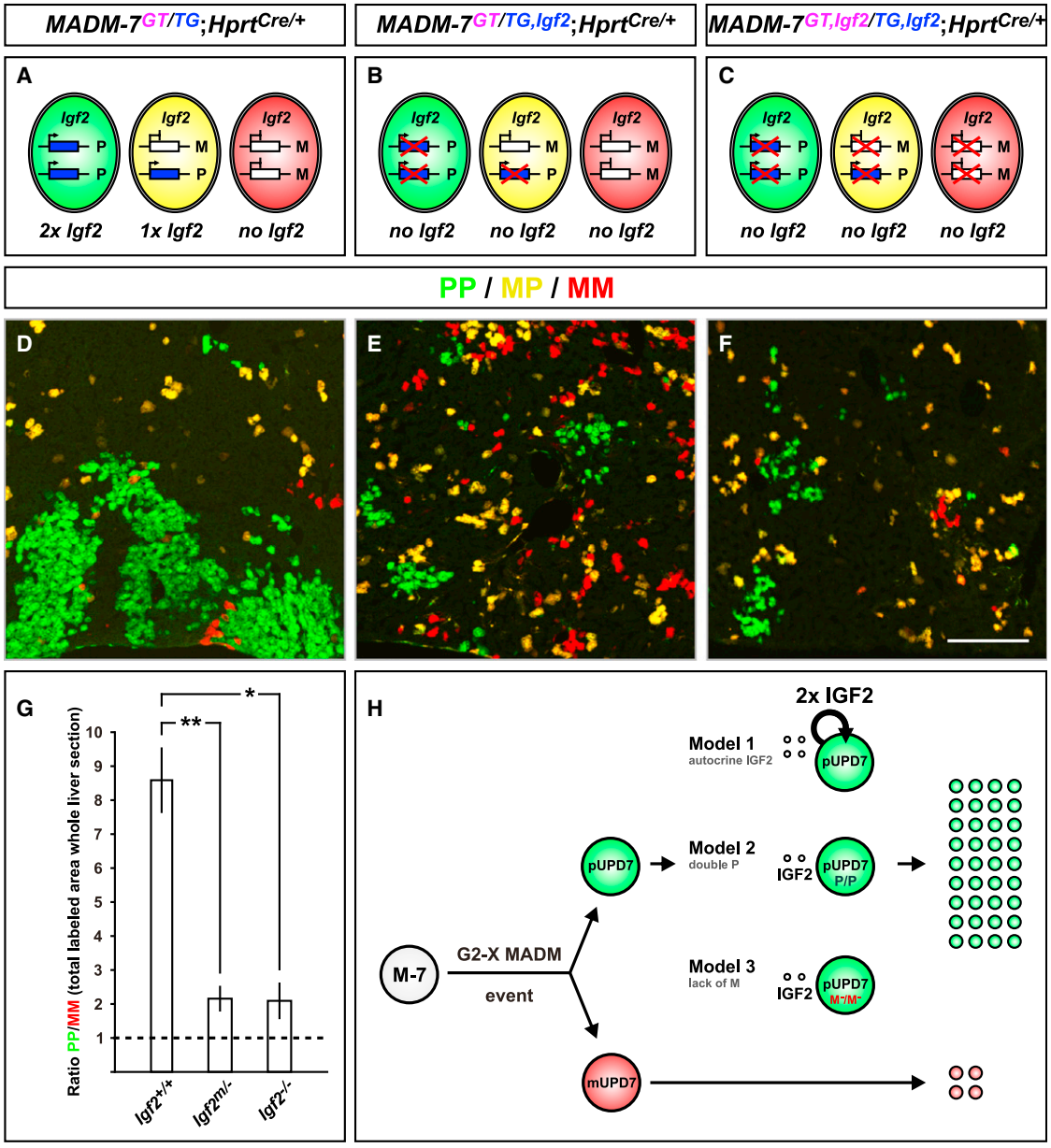

Figure 4. *Igf2* Accounts for Most of the Paternal Dominance in Chromosome 7 UPD

(A–C) Schematic of *Igf2* expression in *MADM-7*$^{GT/TG}$;*Hprt-Cre*$^{+/-}$. (A) Control-MADM-7. (B) *Igf2* mutation on paternal chromosome. (C) *Igf2* mutation on both paternal and maternal chromosomes. Note that due to *Igf2* imprinting, most cells in (B) do not express *Igf2*.

(D–F) Labeling of uniparental chromosome 7 disomy (PP cells are green, and MM cells are red) in P21 control, paternal *Igf2* mutant, or homozygous *Igf2*$^{-/-}$ mutant MADM animals corresponding to the schemes in (A–C). Scale bar, 110 μm.

(G) Quantification of PP/MM ratio in whole-liver sections from P21 MADM animals with genotypes indicated. Values represent mean ± SEM. *$p < 0.05$ and **$p < 0.01$.

(H) Three possible models to account for expansion of cells with unipaternal disomy in sparsely generated MADM-7 clones in wild-type animal. Assuming the crossing scheme in Figure 1A, cells with unipaternal chromosome 7 disomy (pUPD7) are labeled in green and cells with unimaternal chromosome 7 disomy (mUPD7) in red upon a G2-X MADM event. Green pUPD7 cells express a double dose of *Igf2* and P factor(s) but lack M factor(s), where P or M factors represent additional imprinted genes on chromosome 7 that could act cell autonomously to promote or inhibit IGF2 signaling, respectively. In Model 1, IGF2 (double dose) signals strictly autocrine to only pUPD7, but not to mUPD7. In Model 2, the double dose of additional imprinted P factor(s) acts in concert with secreted IGF2 to convey the growth advantage in pUPD7. In Model 3, the lack of M factor(s), which normally would tune down the IGF2 signal to a certain extent, promotes increased IGF2 growth signaling in pUPD7 cells. The cell-type specificity of UPD7 effects we observed may be a consequence of cell-type-specific expression of the M or P factors, or cell-type-specific interactions of these factors with IGF2.

See also Figures S3 and S4.

expressed M factor acts cell autonomously to negatively regulate IGF2 signal transmission. In unipaternal chromosome 7 disomy cells, the lack of the negative M factor results in greatly amplified IGF2 growth signaling.

In both the second and third possibilities above, the additional chromosome 7 P or M imprinted factors contribute, at most, a 2-fold difference independent of IGF2, and their major actions are manifested in the context of cell-autonomous IGF2 signal transmission. We favor the third model because it requires the least number of assumptions; indeed, *Cdkn1c* could represent an attractive candidate for the M factor because genetic interactions have been demonstrated between *Igf2* and *Cdkn1c* (Caspary et al., 1999).

Although *Igf2* displays a highly specific expression pattern in the brain, it is broadly expressed in peripheral embryonic tissues such as the liver, lung, and heart (Davies et al., 2002; DeChiara et al., 1991; Lehtinen et al., 2011). Because we have only detected a significant proliferation advantage in the liver and lung, but not in the heart or the brain, it is highly unlikely that the cell-type-specific effect of imprinting is accounted for by tissue-specific *Igf2* expression patterns. Rather, the tissue specificity of the imprinting effect is likely caused by tissue-specific expression of the M or P factors, or their tissue-specific interactions with IGF2.

Conclusions

We have used the MADM strategy to create, and concomitantly visualize with distinct fluorescent colors, cells with unipaternal and unimaternal near whole-chromosomal disomy. Consequently, it is possible to assay the phenotype of genomic imprinting at the single-cell resolution in virtually any tissue or organ and potentially for every chromosome in the mouse. The results from MADM of chromosome 7 and chromosome 12 revealed chromosomal as well as cell-type-specific imprinting phenotypes. The cell-type specificity of genomic imprinting indicates that certain genes exploit parentally controlled expression regulation in order to fulfill their appropriate physiological functions.

A salient advantage of the MADM method is the controlled generation of defined unipaternal and unimaternal disomic cells that are labeled by two distinct fluorescent colors at the single-cell resolution. This provides a sensitive means to detect phenotypes for homozygosing imprinted genes controlling cell proliferation (such as *Igf2* presented in our study), size, and morphogenesis. An important feature is that MADM-induced UPD cells always display the combined phenotype of the entire cohort of imprinted genes located on a particular chromosome. This could be a limitation when it comes to identifying specific genes on the chromosome that contribute to the imprinting phenotypes. Therefore, the MADM approach complements rather than replaces conventional and/or conditional knockout experiments to study the function of imprinted genes. We presented an example of combining MADM to analyze whole-chromosome UPD with mutation in a selected candidate gene, *Igf2*, and deduced the quantitative contribution of *Igf2* to the imprinting effect of the entire chromosome.

Finally, MADM analysis has been critical to study cell-autonomous functions of candidate genes (besides *Igf2* described in this study) in cell proliferation, neuronal migration, dendrite morphogenesis, and tumor growth (Espinosa et al., 2009; Hippenmeyer et al., 2010; Liu et al., 2011; Muzumdar et al., 2007). The establishment of MADM cassettes on chromosome 7 and chromosome 12 now allows mosaic analysis of a vast majority of genes (~2,500 on chromosome 7, and ~950 on chromosome 12) on two new chromosomes in addition to our previous efforts (Hippenmeyer et al., 2010; Tasic et al., 2012; Zong et al., 2005). Together, MADM-7 and MADM-12 almost double the total number of mouse genes that can be subjected to MADM analysis.

EXPERIMENTAL PROCEDURES

Generation of *MADM-7* and *MADM-12* Mice and Mouse Genetic Techniques

MADM-7 and MADM-12 mice were generated following a previously described strategy (Hippenmeyer et al., 2010). In brief, for MADM-7 and MADM-12-targeting constructs, we identified suitable genomic loci on chromosome 7 (*Hipp7* located at 2.13cM; ~0.7 kb downstream of exon 5 of the *Rps9* gene) and chromosome 12 (*John12* located at 1.71cM; ~16 kb downstream of exon 1 of the *Rab10* gene). The *Hipp7* and *John12* genomic loci were cloned, *GT* and *TG* MADM cassettes (Hippenmeyer et al., 2010; Liu et al., 2011) inserted, and targeting vectors constructed using standard molecular biology procedures (details are available upon request). Linearized targeting vectors were then electroporated into R1 ES cells, and two correctly targeted GT and TG clones for each MADM-7 and MADM-12, respectively, were injected into blastocysts to generate chimeric mice. Homozygous *MADM-7*$^{GT/GT}$, *MADM-7*$^{TG/TG}$, *MADM-12*$^{GT/GT}$, *MADM-12*$^{TG/TG}$, and transheterozygous *MADM-7*$^{GT/TG}$ and *MADM-12*$^{GT/TG}$ were born at Mendelian frequencies, had a normal lifespan, were fertile, showed no obvious averse phenotype, and did not exhibit GFP/tdTomato marker expression in the absence of Cre recombinase.

Heterozygote *Igf2*$^{+/-}$ (DeChiara et al., 1990), *βactin-CreER*$^{+/-}$ (Guo et al., 2002), and hemizygote *Hprt*$^{Cre/Y}$ (Tang et al., 2002) mice have been described. Timed pregnancies were set up to generate embryos at defined developmental stages. For the generation of recombinant *MADM-7*$^{GT,Igf2/TG}$ or *MADM-7*$^{GT/TG,Igf2}$, we followed a standard breeding strategy as previously described (Hippenmeyer et al., 2010). The MADM experiments described in this study were carried out in mixed 129/C57Bl6/CD1 genetic background, and all experimental procedures were carried out in accordance with the Administrative Panel on Laboratory Animal Care protocol and the institutional guidelines by the Veterinary Service Center at Stanford University. *MADM-7*^{GT}, *MADM-7*^{TG}, *MADM-12*^{GT}, and *MADM-12*^{TG} mice are available at Jackson Laboratory Repository (http://jaxmice.jax.org) with the following JAX Stock Numbers: 021457, *MADM-7*^{GT}; 021458, *MADM-7*^{TG}; 021460, *MADM-12*^{GT}; and 021461, *MADM-12*^{TG}.

Analysis of Marker Expression in MADM Animals

Experimental MADM mice at various ages were perfused, and organs were removed and processed for cryosections essentially as described (Hippenmeyer et al., 2010). Typically, we isolated the whole brain, heart, and the largest leaflets of the lung and liver from postnatal mice. Whole embryos were isolated and left intact for processing except that the body was separated from the head, and the limbs were removed. The brain, heart, and lung were cryosectioned sagittally at 60 μm (brain) and 14 μm (heart and lung); coronal sections were acquired from the liver at 14 μm. The fluorescent tdTomato and GFP signals were usually not amplified by antibody staining, but tissue sections were stained with DAPI (Invitrogen) to visualize nuclei and confocal images acquired using a LSM 510 (Zeiss).

Generation and Analysis of MADM Clones in Liver

For the induction of G2-X MADM clones in liver, we set up timed pregnancies, injected TM intraperitoneally at E12, and isolated embryos at E16. Embryos were fixed in 4% PFA/PB overnight, cryoprotected in 30% sucrose/PBS,

embedded in OCT, and sectioned in the sagittal plane at 30 μm. The frequency of MADM clone generation was extremely low and varied between cohorts with slightly different genetic background.

Computation of PP/MM Ratios

Pyramidal cells in hippocampal area CA1 were counted in confocal images from 16 (*MADM-7*$^{GT/TG}$;*Hprt-Cre*$^{+/-}$) and 11 (*MADM-12*$^{GT/TG}$;*Hprt-Cre*$^{+/-}$) cryosections (derived from three animals for each genotype) encompassing the whole CA1 area. Purkinje cells in cerebella were counted in all consecutive sections from four (*MADM-7*$^{GT/TG}$;*Hprt-Cre*$^{+/-}$) and three (*MADM-12*$^{GT/TG}$;*Hprt-Cre*$^{+/-}$) entire half-brains derived from more than two animals each. For quantification of heart cardiomyocyte and liver hepatocyte populations, the green (GFP) and red (tdTomato) MADM signals were first extracted manually from confocal images derived from cryosections to separate them from the yellow GFP^{+}/tdTomato^{+} signal. The total areas of green and red signals, respectively, were then computed from binary images using a custom MATLAB script. The geometric means ± SEM of the paternal/maternal ratios were calculated in Excel, and significance was determined using Student's t test: *$p < 0.05$ and **$p < 0.01$.

SUPPLEMENTAL INFORMATION

Supplemental Information includes four figures and can be found with this article online at http://dx.doi.org/10.1016/j.celrep.2013.02.002.

LICENSING INFORMATION

ACKNOWLEDGMENTS

We thank H. Zong for FLLFL MADM cassettes and discussions about MADM; Y. Chen-Tsai and the Stanford Transgenic Facility for generating knockin mice; A. Efstratiadis and C. Walsh for providing *Igf2* mutant mice; C. Manalac, J. Zhong, K. Jaeckle, C. Nguyen, and M. Shu for technical support; and H. Chang, N. Makki, B. Weissbourd, and T. Mosca for helpful comments on the manuscript. This work was supported by the European Molecular Biology Organization ALTF 851-2005 (to S.H.), Human Frontier Science Program Organization LT00805/2006-L (to S.H.), Swiss National Science Foundation PA00P3_124160 and PA00P3_136482 (to S.H.), and NIH grants R01-NS050835 (to L.L.) and R01-HD060579 (R.L.J.). L.L. is an investigator of the Howard Hughes Medical Institute.

Received: October 25, 2012
Revised: January 5, 2013
Accepted: February 1, 2013
Published: February 28, 2013

REFERENCES

Barlow, D.P. (2011). Genomic imprinting: a mammalian epigenetic discovery model. Annu. Rev. Genet. *45*, 379–403.

Bartolomei, M.S., and Ferguson-Smith, A.C. (2011). Mammalian genomic imprinting. Cold Spring Harb. Perspect. Biol. *3*, a002592.

Bartolomei, M.S., Zemel, S., and Tilghman, S.M. (1991). Parental imprinting of the mouse H19 gene. Nature *351*, 153–155.

Barton, S.C., Surani, M.A., and Norris, M.L. (1984). Role of paternal and maternal genomes in mouse development. Nature *311*, 374–376.

Caspary, T., Cleary, M.A., Perlman, E.J., Zhang, P., Elledge, S.J., and Tilghman, S.M. (1999). Oppositely imprinted genes p57(Kip2) and igf2 interact in a mouse model for Beckwith-Wiedemann syndrome. Genes Dev. *13*, 3115–3124.

Cattanach, B.M., and Kirk, M. (1985). Differential activity of maternally and paternally derived chromosome regions in mice. Nature *315*, 496–498.

Chao, W., and D'Amore, P.A. (2008). IGF2: epigenetic regulation and role in development and disease. Cytokine Growth Factor Rev. *19*, 111–120.

Davies, K., Bowden, L., Smith, P., Dean, W., Hill, D., Furuumi, H., Sasaki, H., Cattanach, B., and Reik, W. (2002). Disruption of mesodermal enhancers for Igf2 in the minute mutant. Development *129*, 1657–1668.

DeChiara, T.M., Efstratiadis, A., and Robertson, E.J. (1990). A growth-deficiency phenotype in heterozygous mice carrying an insulin-like growth factor II gene disrupted by targeting. Nature *345*, 78–80.

DeChiara, T.M., Robertson, E.J., and Efstratiadis, A. (1991). Parental imprinting of the mouse insulin-like growth factor II gene. Cell *64*, 849–859.

Espinosa, J.S., Wheeler, D.G., Tsien, R.W., and Luo, L. (2009). Uncoupling dendrite growth and patterning: single-cell knockout analysis of NMDA receptor 2B. Neuron *62*, 205–217.

Feinberg, A.P. (2007). Phenotypic plasticity and the epigenetics of human disease. Nature *447*, 433–440.

Ferguson-Smith, A.C. (2011). Genomic imprinting: the emergence of an epigenetic paradigm. Nat. Rev. Genet. *12*, 565–575.

Ferguson-Smith, A.C., Cattanach, B.M., Barton, S.C., Beechey, C.V., and Surani, M.A. (1991). Embryological and molecular investigations of parental imprinting on mouse chromosome 7. Nature *351*, 667–670.

Ferrón, S.R., Charalambous, M., Radford, E., McEwen, K., Wildner, H., Hind, E., Morante-Redolat, J.M., Laborda, J., Guillemot, F., Bauer, S.R., et al. (2011). Postnatal loss of Dlk1 imprinting in stem cells and niche astrocytes regulates neurogenesis. Nature *475*, 381–385.

Garfield, A.S., Cowley, M., Smith, F.M., Moorwood, K., Stewart-Cox, J.E., Gilroy, K., Baker, S., Xia, J., Dalley, J.W., Hurst, L.D., et al. (2011). Distinct physiological and behavioural functions for parental alleles of imprinted Grb10. Nature *469*, 534–538.

Guo, C., Yang, W., and Lobe, C.G. (2002). A Cre recombinase transgene with mosaic, widespread tamoxifen-inducible action. Genesis *32*, 8–18.

Hatada, I., and Mukai, T. (1995). Genomic imprinting of p57KIP2, a cyclin-dependent kinase inhibitor, in mouse. Nat. Genet. *11*, 204–206.

Hippenmeyer, S., Youn, Y.H., Moon, H.M., Miyamichi, K., Zong, H., Wynshaw-Boris, A., and Luo, L. (2010). Genetic mosaic dissection of Lis1 and Ndel1 in neuronal migration. Neuron *68*, 695–709.

Lehtinen, M.K., Zappaterra, M.W., Chen, X., Yang, Y.J., Hill, A.D., Lun, M., Maynard, T., Gonzalez, D., Kim, S., Ye, P., et al. (2011). The cerebrospinal fluid provides a proliferative niche for neural progenitor cells. Neuron *69*, 893–905.

Liu, C., Sage, J.C., Miller, M.R., Verhaak, R.G., Hippenmeyer, S., Vogel, H., Foreman, O., Bronson, R.T., Nishiyama, A., Luo, L., and Zong, H. (2011). Mosaic analysis with double markers reveals tumor cell of origin in glioma. Cell *146*, 209–221.

Mabb, A.M., Judson, M.C., Zylka, M.J., and Philpot, B.D. (2011). Angelman syndrome: insights into genomic imprinting and neurodevelopmental phenotypes. Trends Neurosci. *34*, 293–303.

Matsuoka, S., Edwards, M.C., Bai, C., Parker, S., Zhang, P., Baldini, A., Harper, J.W., and Elledge, S.J. (1995). p57KIP2, a structurally distinct member of the p21CIP1 Cdk inhibitor family, is a candidate tumor suppressor gene. Genes Dev. *9*, 650–662.

McGrath, J., and Solter, D. (1984). Completion of mouse embryogenesis requires both the maternal and paternal genomes. Cell *37*, 179–183.

McLaughlin, K.J., Kochanowski, H., Solter, D., Schwarzkopf, G., Szabó, P.E., and Mann, J.R. (1997). Roles of the imprinted gene Igf2 and paternal duplication of distal chromosome 7 in the perinatal abnormalities of androgenetic mouse chimeras. Development *124*, 4897–4904.

Muzumdar, M.D., Luo, L., and Zong, H. (2007). Modeling sporadic loss of heterozygosity in mice by using mosaic analysis with double markers (MADM). Proc. Natl. Acad. Sci. USA *104*, 4495–4500.

Nicholls, R.D., and Knepper, J.L. (2001). Genome organization, function, and imprinting in Prader-Willi and Angelman syndromes. Annu. Rev. Genomics Hum. Genet. *2*, 153–175.

Stanger, B.Z. (2008). Organ size determination and the limits of regulation. Cell Cycle *7*, 318–324.

Stanger, B.Z., Tanaka, A.J., and Melton, D.A. (2007). Organ size is limited by the number of embryonic progenitor cells in the pancreas but not the liver. Nature *445*, 886–891.

Surani, M.A., Barton, S.C., and Norris, M.L. (1984). Development of reconstituted mouse eggs suggests imprinting of the genome during gametogenesis. Nature *308*, 548–550.

Tang, S.H., Silva, F.J., Tsark, W.M., and Mann, J.R. (2002). A Cre/loxP-deleter transgenic line in mouse strain 129S1/SvImJ. Genesis *32*, 199–202.

Tasic, B., Miyamichi, K., Hippenmeyer, S., Dani, V.S., Zeng, H., Joo, W., Zong, H., Chen-Tsai, Y., and Luo, L. (2012). Extensions of MADM (mosaic analysis with double markers) in mice. PLoS One *7*, e33332.

Wilkinson, L.S., Davies, W., and Isles, A.R. (2007). Genomic imprinting effects on brain development and function. Nat. Rev. Neurosci. *8*, 832–843.

Williamson, C.M., B.A., Thomas, S., Beechey, C.V., Hancock, J., Cattanach, B.M., and Peters, J. (2013). MRC Harwell, Oxfordshire. World Wide Web Site-Mouse Imprinting Data and References. http://www.har.mrc.ac.uk/research/genomic_imprinting/.

Zong, H., Espinosa, J.S., Su, H.H., Muzumdar, M.D., and Luo, L. (2005). Mosaic analysis with double markers in mice. Cell *121*, 479–492.

Cell PRESS
Open ACCESS

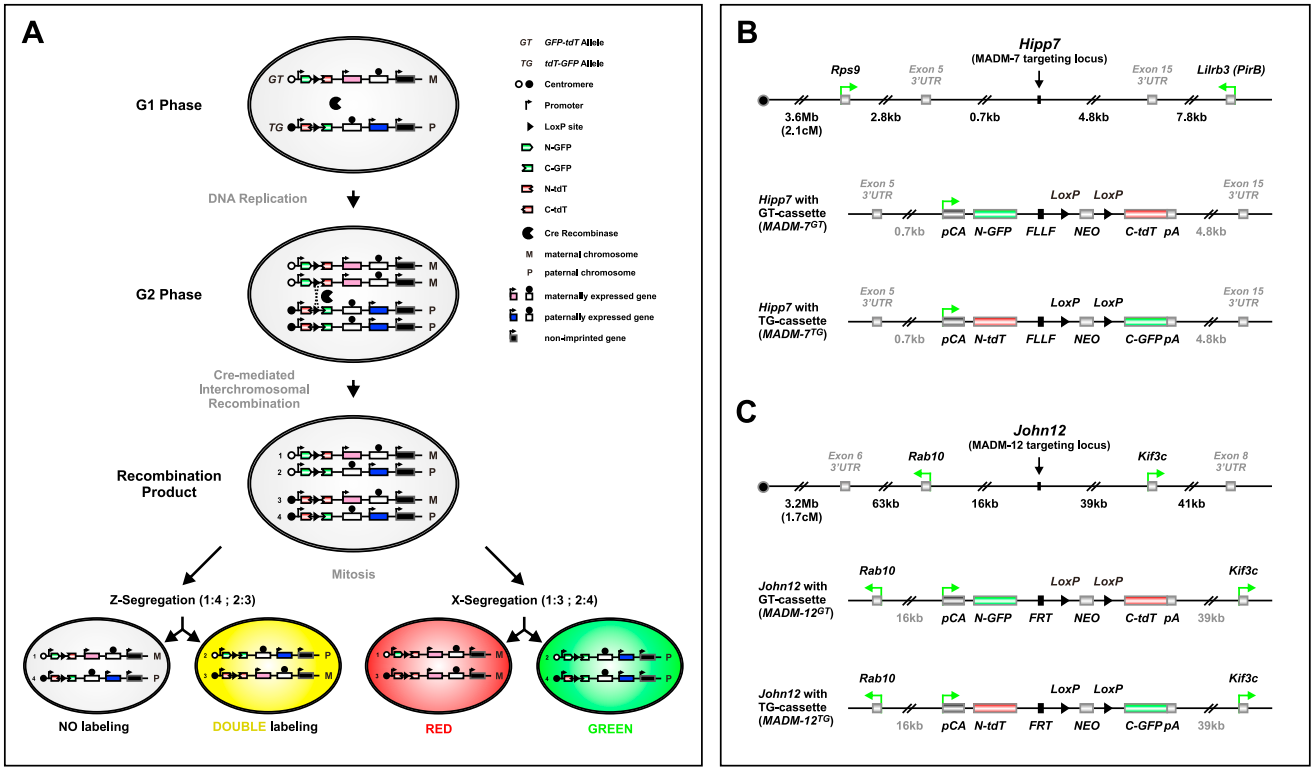

Figure S1. MADM Principle for Imprinted Genes and Targeting Strategy to Generate MADM-7 and MADM-12, Related to Figure 1

(A) MADM is based upon Cre/LoxP-dependent interchromosomal recombination whereby two reciprocal chimeric marker genes (GT and TG) are reconstituted. Recombination in postmitotic cells or during the G1 phase of the cell cycle reconstitutes both green and red markers in the same cell, and produces yellow cells without altering the genotype (not shown). Recombination in G2 with both reconstituted marker genes (and corresponding chromosomes) segregating to the same daughter cell upon mitosis (Z-Segregation) also does not alter the genotype, and produces one yellow cell (left branch). In contrast, recombination in G2 followed by X-Segregation where the two recombinant chromosomes segregate into distinct daughter cells, results in each cell expressing either GFP (green) or tdTomato (tdT, red), and displays near complete uniparental chromosomal disomy (UPD, right branch). If the GT MADM cassette is inherited from the mother (M) and the TG MADM cassette from the father (P), as shown in this schematic, red cells harbor unimaternal chromosomal disomy (MM) and green cells unipaternal chromosomal disomy (PP). Consequently, maternally expressed genes (pink) are expressed at twice the normal dose and paternally expressed genes (blue) are not expressed in red cells with unimaternal disomy. By contrast, paternally expressed genes are expressed at twice the normal dose and maternally expressed genes are not expressed in green, unipaternal disomy cells. Thus, genes subject to imprinting are differentially expressed depending on the UPD. Non-imprinted genes (black) are not affected. Symbols used in this schematic and in Figure 1A are detailed in the key.

(B) Targeting of the *Hipp7* genomic locus with GT and TG MADM cassettes, respectively. Top panel: the genomic organization of the *Hipp7* locus. The insertion site (MADM-7 targeting locus) is located ~0.7kb telomeric to exon 5 of the *Rps9* gene and ~4.8kb centromeric to exon 15 of the *Lilrb3* (*PirB*) gene. Middle panel: the *Hipp7* locus with inserted GT cassette (*MADM-7*^{GT}). Bottom panel: the *Hipp7* locus with inserted TG cassette (*MADM-7*^{TG}).

(C) Targeting of *John12* genomic locus with GT and TG MADM cassettes, respectively. Top panel: the genomic organization of the *John12* locus. The insertion site (MADM-12 targeting locus) is located ~16kb downstream of exon 1 of the *Rab10* gene and ~39kb upstream of exon 1 of the *Kif3c* gene. Middle panel: the *John12* locus with inserted GT cassette (*MADM-12*^{GT}). Bottom panel: the *John12* locus with inserted TG cassette (*MADM-12*^{TG}).

GT and TG MADM cassettes have been described: for cassettes in MADM-12 see (Hippenmeyer et al., 2010); cassettes for MADM-7 include LoxP - FRT-Lox5171-Lox2272-FRT – (Liu et al., 2011; Tasic et al., 2012).

Cell PRESS
Open ACCESS

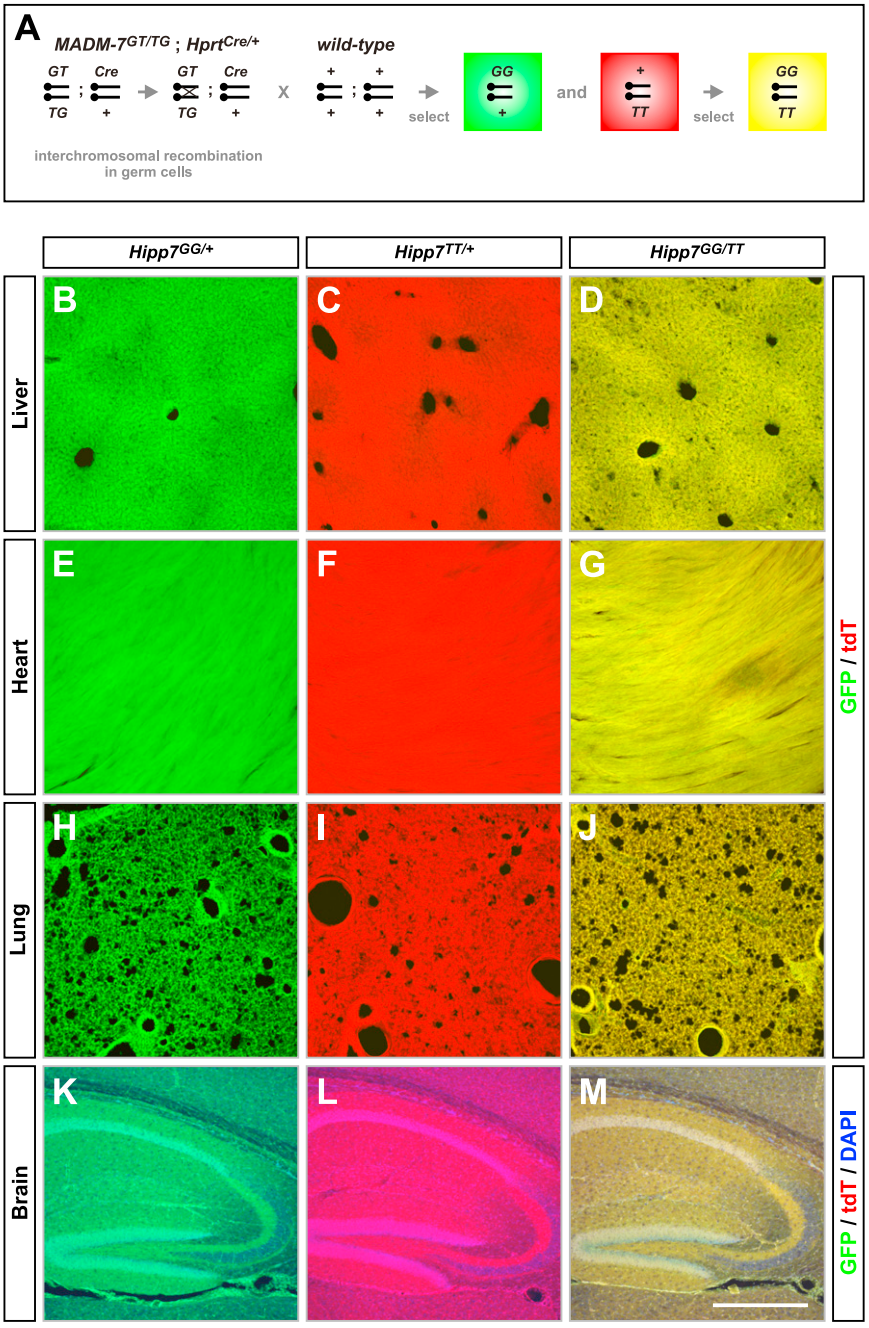

Figure S2. Biallelic and Global Expression of MADM from Genomic *Hipp7* Locus, Related to Figure 2

(A) Breeding strategy to generate GG (green, $Hipp7^{GG/+}$), TT (red, $Hipp7^{TT/+}$) and GG/TT (yellow, $Hipp7^{GG/TT}$) animals with reconstituted MADM marker genes. First, $MADM\text{-}7^{GT/TG}$;$Hprt^{Cre/+}$ animals were mated to wild-type. 'Green GG' ($Hipp7^{GG/+}$) and 'red TT' ($Hipp7^{TT/+}$) offspring animals (derived from germ cells where interchromosomal recombination has led to reconstituted GG and TT markers) were selected. $Hipp7^{GG/+}$ were then crossed to $Hipp7^{TT/+}$ to generate $Hipp7^{GG/TT}$ animals.

(B–M) Marker expression from the *Hipp7* locus in $Hipp7^{GG/+}$ (B, E, H, and K), $Hipp7^{TT/+}$ (C, F, I, and L) and $Hipp7^{GG/TT}$ (D, G, J, and M) in liver (B–D), heart (E–G), lung (H–J) and brain (hippocampus; K–M) at P21. In all images, both green and red channels from confocal microscopy were acquired and shown. Thus, $Hipp7^{GG/+}$ only express GFP; $Hipp7^{TT/+}$ only express tdT; $Hipp7^{GG/TT}$ express both with similar intensity, hence all cells are yellow. DAPI delineates CA1, CA3 and dentate gyrus regions in (K-M). Scale bar: 500 μm.

Cell PRESS
Open ACCESS

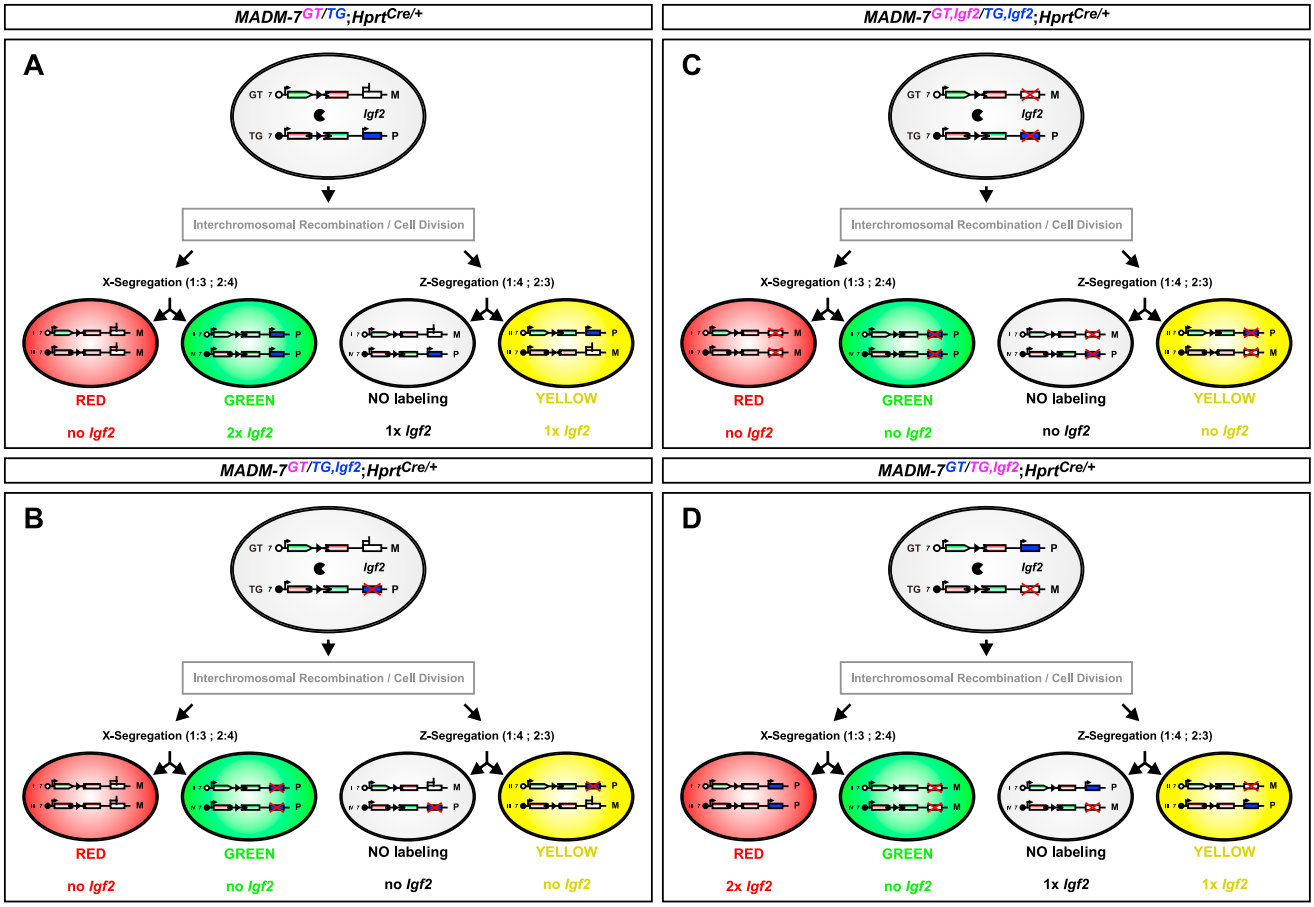

Figure S3. MADM Scheme for Analyzing the Imprinted Gene *Igf2*, Related to Figure 4

(A) Control MADM scheme (see Figure S1 for symbols). Imprinting (silencing) of the maternal *Igf2* allele (white) and expression from the paternal allele (blue) are indicated in a cell before MADM is induced. The GT or TG cassette is located on the maternal (M) or paternal (P) chromosome, respectively. Different MADM events would produce labeled cells with the *Igf2* genotypes shown at the bottom: 2x *Igf2* for green cells, 1x *Igf2* for yellow cells and no *Igf2* for red cells.

(B) MADM scheme for paternal transmission of the mutant *Igf2* allele. Because the maternal allele should be silenced, no *Igf2* expression is predicted in green, red, and yellow cells.

(C) MADM scheme for transmission of the mutant *Igf2* allele from both parents. No *Igf2* expression occurs in green, red, and yellow cells.

(D) MADM scheme for maternal transmission of the mutant *Igf2* allele. Because the maternal allele should be silenced in any case, the *Igf2* expression pattern is predicted to resemble that of control MADM (A).

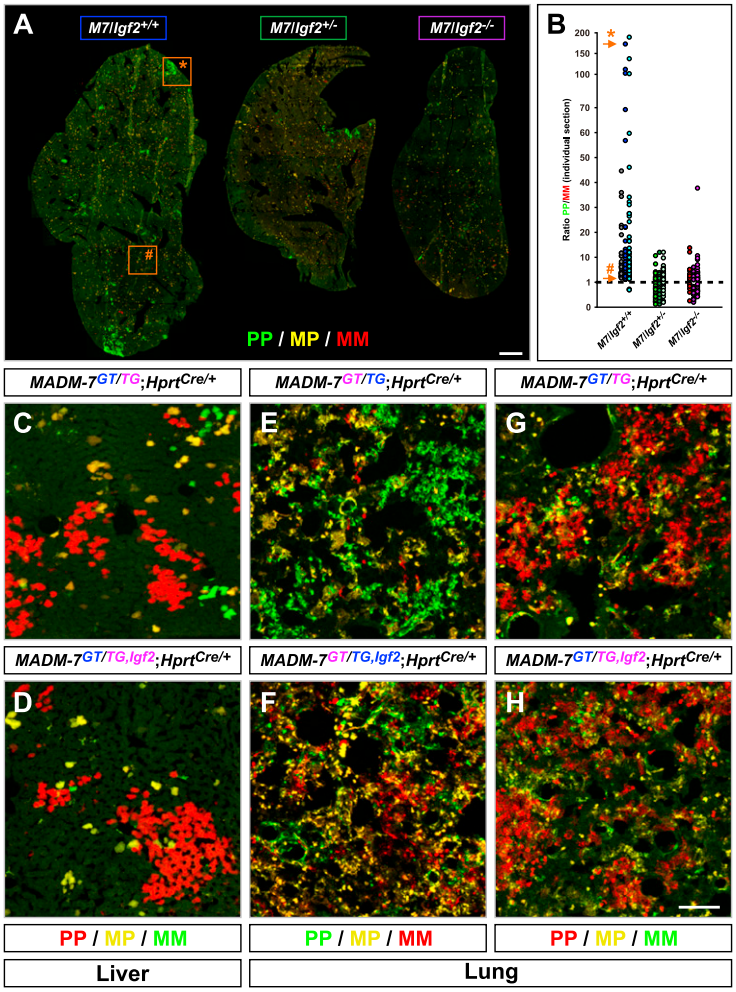

Figure S4. Detailed Analysis and Quantification of PP/MM Ratio in *Igf2*-MADM-7 Tissues, Related to Figure 4

(A) Representative images of whole liver sections assembled from individual confocal scans from P21 *MADM-7*$^{GT/TG}$;*Hprt*$^{Cre/+}$ (left; *Igf2*$^{+/+}$), *MADM-7*$^{GT/TG,Igf2}$;*Hprt*$^{Cre/+}$ (middle; *Igf2*$^{m/-}$, *Igf2* mutation from father), and *MADM-7*$^{GT,Igf2/TG,Igf2}$;*Hprt*$^{Cre/+}$ (right; *Igf2*$^{-/-}$, homozygous *Igf2* mutant). In all cases, green (GFP) cells harbor unipaternal Chr.7 disomy (PP), red (tdT) cells unimaternal Chr.7 disomy (MM) and yellow (GFP/tdT) cells are wild-type (PM). Note that the liver sections are significantly smaller in *Igf2*$^{m/-}$ and *Igf2*$^{-/-}$ when compared to *Igf2*$^{+/+}$, consistent with IGF2 being required for normal growth (DeChiara et al., 1990).

(B) Quantification of PP/MM ratios in P21 *Igf2*$^{+/+}$, *Igf2*$^{m/-}$, and *Igf2*$^{-/-}$ MADM samples. Every data point represents the ratio of one confocal image (25-56 per compiled liver section from individual animals/genotypes). The large numeric variance reflects the variable sizes of clones with MADM labeling. Two extreme data points are highlighted with a star (indicates the highest) and square (lowest) PP/MM ratio in *Igf2*$^{+/+}$. One representative whole liver section was quantified from n = 3 individual animals and per genotype.

(C and D) No mitigation of paternal dominance in MADM-7 liver with maternal transmission of *Igf2* mutation. (C) Representative section of P21 liver with GT inherited from father and TG inherited from mother (*MADM-7*$^{GT/TG}$;*Hprt*$^{Cre/+}$). Thus, cells with unipaternal Chr.7 disomy (PP) appear in red (labeled by tdT), and are present at increased numbers when compared to cells with unimaternal Chr.7 disomy (MM) in green (labeled by GFP). (D) Representative section of P21 liver in *MADM-7*$^{GT/TG,Igf2}$;*Hprt*$^{Cre/+}$ with GT inherited from father, and TG and the *Igf2* mutation inherited from the mother. See Figure S3D for detailed MADM scheme. Note that red MM cells outnumber green PP cells similar as in (C), indicating that maternal inheritance of the *Igf2* mutation has no functional relevance (due to imprinting status) since the paternal *Igf2* allele is still overexpressed at double dose in red PP cells.

(E–H) Diminished paternal dominance in MADM-7 lung with paternal but not maternal transmission of *Igf2* mutation. (E) Representative section of P21 lung with TG inherited from the father and GT inherited from the mother. Cells with unipaternal Chr.7 disomy (PP) are labeled in green by GFP expression, and are overabundant when compared to cells with unimaternal Chr.7 disomy (MM) labeled in red by tdT expression. (F) Paternal transmission of *Igf2* mutation results in reduced paternal dominance as seen by the reduced number of green PP cells compared with (E). (G) Representative section of P21 lung with GT inherited from father and TG inherited from mother. Cells with unipaternal Chr.7 disomy (PP) are labeled in red by tdT expression, and are overabundant when compared to cells with unimaternal Chr.7 disomy (MM) labeled in green by GFP expression. (H) Maternal transmission of *Igf2* mutation does not affect paternal dominance as seen by similar overabundance of red cells as in (G).

Scale bars: 1mm (A); 100 μm (C–H).